Nuclear Instruments and Methods in Physics Research A 614 (2010) 453–460

Contents lists available at ScienceDirect

Nuclear Instruments and Methods in Physics Research A

journal homepage: www.elsevier.com/locate/nima

A semi-analytic approximation of charge induction in monolithic pixelated CdZnTe radiation detectors

Derek S. Bale *

eV Microelectronics, a Division of Endicott Interconnect Technologies, Inc. 373 Saxonburg Blvd., Saxonburg, PA 16056, USA

ARTICLE INFO

Article history:
Received 7 October 2009
Accepted 15 December 2009
Available online 22 December 2009

Keywords:
CdZnTe
CZT
Solid-state gamma-ray detection
X-ray imaging
Pixelated semiconductor radiation detector

ABSTRACT

A semi-analytic approximation to the weighting potential within monolithic pixelated CdZnTe radiation detectors is presented. The approximation is based on solving the multi-dimensional Laplace equation that results upon replacing rectangular pixels with equal-area circular pixels. Further, we utilize the simplicity of the resulting approximate weighting potential to extend the well-known Hecht equation, describing charge induction in a parallel plate detector, to that approximating the multi-dimensional charge induction within a pixelated detector. These newly found expressions for the weighting potential and charge induction in a pixelated detector are compared throughout to full 3D electrostatic and monte carlo simulations using eVDSIM (**eV** Microelectronics **D**evice **SIM**ulator). The semi-analytic expressions derived in this paper can be evaluated quickly, and can therefore be used to efficiently reduce the size and dimensionality of the parameter space on which a detailed 3D numerical analysis is needed for pixelated detector design in a wide range of applications.

1. Introduction

The wide band gap and high mean atomic number of semi-insulating cadmium zinc telluride (CdZnTe) make it an attractive material candidate for the room-temperature detection of x- and γ-rays in a wide range of spectroscopic and imaging applications. Despite an impressive improvement in single-crystal growth techniques that have produced high electron transport material (i.e. electron mobility-lifetime product $\mu_e\tau_e > 10^{-2}\,\text{cm}^2\,\text{V}^{-1}$) over the past decade, [1,2] hole trapping at impurities and crystal defects keep the hole transport properties lower (i.e. hole mobility-lifetime product $\mu_h\tau_h \sim (0.3-10)\times 10^{-5}\,\text{cm}^2\,\text{V}^{-1}$). Because of this, there has been a major effort to design single-polarity spectroscopic CdZnTe detectors that are insensitive to the transport of holes. These designs include detectors based on coplanar grid, [3–5] 2D strip, [6,7] 2D pixel array, [8,9] Frisch ring, [10,11] and quasi-hemispherical [12–14] electrode geometries.

One consequence of having to develop multi-element single-polarity detectors is that the design for optimal charge collection is more challenging than that for a simple parallel plate (i.e., planar) detector. Though charge induction within a planar detector is well known, for comparison purposes to formulae derived in what follows we write it here in terms of a single-carrier functional defined by

$$\mathcal{F}_{\parallel}(z_0,t;\tau,\lambda)=\lambda\begin{cases}1-\exp(-t/\tau) & t\le\tau_{\rm tr}\\ 1-\exp(-\tau_{\rm tr}/\tau) & t>\tau_{\rm tr}\end{cases} \tag{1}$$

where $\tau_{\rm tr}$ is the carrier time-of-flight that depends on the photon interaction depth z_0, and $\lambda=\mu\tau V/L^2$ is the distance traveled by a carrier in a single trapping time τ, normalized by the detector thickness L. The applied bias voltage has been denoted by V. The functional $\mathcal{F}_{\parallel}$ describes the time-dependent electron contribution to the induced signal when $\mu\tau=\mu_e\tau_e$ and $\tau_{\rm tr}=L(L-z_0)/(\mu_e V)$, and similarly the hole contribution when $\mu\tau=\mu_h\tau_h$ and $\tau_{\rm tr}=Lz_0/(\mu_h V)$. Using $\mathcal{F}_{\parallel}$, we can write the time-dependent signal induced by both electrons and holes in a planar detector as

$$\eta(z_0,t)=\mathcal{F}_{\parallel}(z_0,t;\tau_e,\lambda_e)+\mathcal{F}_{\parallel}(z_0,t;\tau_h,\lambda_h). \tag{2}$$

Upon full transit of each carrier type, the total fraction of induced charge is described by the well known Hecht relation, [15]

$$\mathcal{H}(z_0)=\lambda_e\left[1-\exp\left(-\frac{1-z_0/L}{\lambda_e}\right)\right]+\lambda_h\left[1-\exp\left(-\frac{z_0}{L\lambda_h}\right)\right] \tag{3}$$

which simply results from evaluating Eq. (2) at $t=\max\{L(L-z_0)/(\mu_e V), Lz_0/(\mu_h V)\}$.

The Hecht equation provides insight into the dependence of charge induction in planar geometry on critical material and detector design parameters. Unfortunately, no such expression exists for the charge induction within single-polarity detectors designed with general multi-element electrode geometries. In this

* Tel.: +1 724 352 6358.
E-mail address: derek.bale@evmicroelectronics.com

0168-9002/$ - see front matter © 2010 Elsevier B.V. All rights reserved.
doi:10.1016/j.nima.2009.12.046

case, the design process often involves a large matrix of 3D numerical simulations to solve for the electrostatic and weighting fields that optimize the charge collection properties of the detector. These simulations typically cover a rather large design parameter space, and are therefore time consuming and generate large amounts of data that must be properly analyzed to pull out the physics that is so naturally apparent in Eq. (3).

Despite the challenges, there are idealized multi-element electrode geometries for which researchers have found analytical solutions to the electrostatic equations. Following Luke's work on single-polarity devices, [3,4] Z. He used the method of separation of variables [16] to derive an analytical expression for the potential distribution within detectors with coplanar strip electrodes. [5] Similarly, following the suggestion of Barrett et al. in Ref. [9] that hole transport can also be suppressed by using 2D segmented (i.e., pixelated) electrodes, Eskin et al. used Fourier transform and Green's function methods to derive the weighting potential within a pixelated detector with negligible gap width given by

$$\phi_w(\mathbf{r},z) = \frac{1}{L^2}\int_{\text{pix}} d^2r' \sum_{n=1}^{\infty} -n\,(-1)^n \sin\left(\frac{n\pi z}{L}\right) K_0\left(\frac{n\pi|\mathbf{r}-\mathbf{r}'|}{L}\right) \tag{4}$$

where K_0 is the zero-order modified Bessel function of the second kind [8]. Unfortunately, except for the 2D case of a strip detector, in practice this integral must be evaluated numerically for 2D pixel geometries. [8] However, similar to a full 3D numerical solution, the discrete evaluation of the integral in Eq. (4) is computationally expensive. Further, representing the weighting potential as a discrete set of numerical values precludes any (semi-)analytical extension of the Hecht Eq. (3) for charge induction in pixelated detectors.

In this work, we seek a simpler, albeit approximate, analytical expression for the weighting potential and charge induction within a pixelated detector. To that end, we replace rectangular pixels with equal-area circular pixels in Section 2 to derive a semi-analytic approximation to the weighting potential within a pixelated CdZnTe radiation detector. In Section 3, we utilize the simplicity of this weighting potential to generalize the Hecht equation to approximate the multi-dimensional charge induction in a pixelated detector. The analytical expressions derived in this paper can be evaluated quickly, and therefore can be used to efficiently reduce the design parameter space on which one must apply a detailed and time-consuming 3D numerical analysis. The accuracy of the newly derived semi-analytic approximations for the weighting potential and charge induction are compared throughout with full 3D electrostatic and monte carlo simulations using eVDSIM (**eV** Microelectronics **D**evice **SIM**ulator) [17].

2. Approximation of the weighting potential

We are interested in approximating the charge induction properties of a monolithic CdZnTe detector with a full metal contact on the cathode at $z=0$, and an $n\times n$ array of pixels on the anode at $z=L$. Such a detector is depicted in Fig. 1 with square pixels of linear dimension w, and a cathode negatively biased to $-V$ Volts. Though Fig. 1 depicts large gaps between the pixels for a visual effect, typical gap sizes on fabricated detectors are $\sim(50-100)\,\mu$m so that the fractional surface area covered by the gaps on a detector with surface area $10\times10\,\text{mm}^2$ is negligible. Therefore, the electric field is uniform and indistinguishable from that of a planar detector throughout most of the detector volume, except within a pixel dimension of the anode plane. The same is not true for the weighting field, and in what follows we derive it approximately.

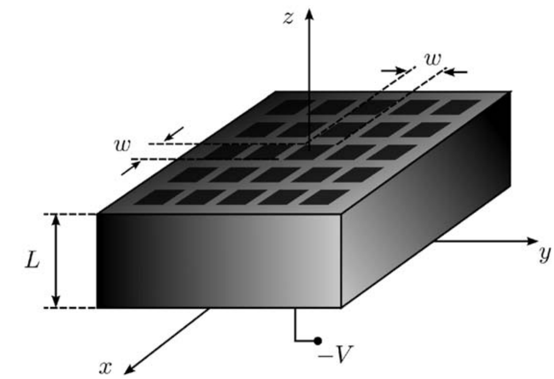

Fig. 1. pixelated CdZnTe radiation detector with thickness L and pixel dimension $w\times w$.

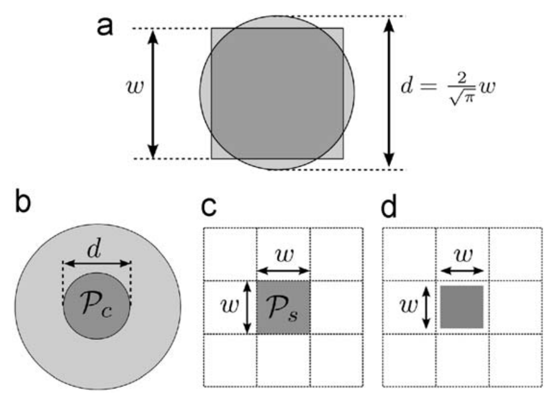

Fig. 2. (a) The square pixel $\mathcal{P}_s$ is replaced with an equal-area circular pixel $\mathcal{P}_c$ with diameter $d=2w/\sqrt{\pi}$ (equal area pixels), (b) detector *DetC0* has zero-gap circular pixel $\mathcal{P}_c$ with diameter d (*DetCO*), (c) detector *DetS0* has zero-gap square pixel $\mathcal{P}_s$ with linear dimension w(*DetSO*), (d) detector *DetS* has square pixel with linear dimension w, but non-zero gap (*DetS*).

2.1. Geometric approximation

In deriving Eq. (4), Eskin et al. employed a zero-gap approximation, together with an assumption that they could neglect electrostatic edge effects and let $n\to\infty$, thereby assuming an infinite 2D plane of pixels. The central nine pixels of this geometry are shown in Fig. 2(c). In the analysis presented here, we follow Eskin et al. and assume zero gap size together with an infinite 2D plane of pixels, however, we replace the square collecting pixel, denoted by $\mathcal{P}_s$ in Fig. 2(c), with an equal-area circular pixel, denoted by $\mathcal{P}_c$ in Fig. 2(b), with diameter given by

$$d = 2R = \frac{2}{\sqrt{\pi}}w. \tag{5}$$

The anode geometry that results in the zero-gap approximation is depicted in Fig. 2(b). Our motivation for the geometrical replacement of $\mathcal{P}_s$ with $\mathcal{P}_c$ stems from the boundary conditions associated with the solution of the weighting potential, ϕ_w. Since $\phi_w=1$ on the collecting pixel $\mathcal{P}_s$, and $\phi_w=0$ on all other non-collecting elements, the resulting radially symmetric Laplace problem only differs from the original problem at points in the set $\mathcal{P}_s\cup\mathcal{P}_c-\mathcal{P}_s\cap\mathcal{P}_c$. Because this set of points is small, so too will be the error generated by such an approximation. The benefit, however, is a simple radially symmetric problem that can be solved exactly using the method of separation of variables [16].